

Random numbers from vacuum fluctuations

Yicheng Shi,^{1,2} Brenda Chng,² and Christian Kurtsiefer^{1,2}

¹Department of Physics, National University of Singapore, 2 Science Drive 3, Singapore, 117542

²Center for Quantum Technologies, National University of Singapore, 3 Science Drive 2, Singapore, 117543

(Dated: 12 July 2016)

We implement a quantum random number generator based on a balanced homodyne measurement of vacuum fluctuations of the electromagnetic field. The digitized signal is directly processed with a fast randomness extraction scheme based on a linear feedback shift register. The random bit stream is continuously read in a computer at a rate of about 480 Mbit/s and passes an extended test suite for random numbers.

I. INTRODUCTION

Various cryptographic schemes, classical or quantum, require high quality and trusted random numbers for key generation and other aspects of the protocols. In order to keep up with data rates in modern communication schemes, these random numbers need to be generated at a high rate¹. Equally, large amounts of random numbers are at the core of Monte Carlo simulations². Algorithmically generated pseudo-random numbers are available at very high rates, but are deterministic by definition and therefore unsuitable for cryptographic purposes. For applications that require unpredictable random numbers, hardware random number generators have been used in the past³ and more recently⁴. These involve measuring noisy physical processes, and conversion of the outcome into random numbers. Since it is either practically (e.g. for thermal noise sources) or fundamentally impossible to predict the outcome of such measurements, these physically generated random numbers are considered “truly” random.

Quantum random number generators (QRNG) belong to a class of hardware random number generators where the source of randomness is the fundamentally unpredictable outcome of quantum measurements. Early QRNGs were based on observing the decay statistics of radioactive nuclei^{5,6}. More recently, similar QRNGs based on Poisson statistics in optical photon detection have been reported^{7–13}. Different schemes use the randomness of a single photon scattered by a beam splitter into either of two output ports^{14,15}. As the reflection/transmission of the photon is intrinsically random due to the quantum nature of the process, the unpredictability of the generated numbers is ensured¹⁶. Other implementations of QRNGs measure the amplified spontaneous emission¹⁷, the vacuum fluctuations of the electromagnetic field^{18–20}, or the intensity^{21,22} and phase noise of different light sources^{23–30}.

In this paper we report on a QRNG based on measuring vacuum fluctuations of a light field as the source of randomness^{18–20}. Such measurements have a very high bandwidth compared to schemes based on photon counting^{7–13}, and have a much simpler optical setup compared to phase noise measurements^{23–30}. Coupled with an effi-

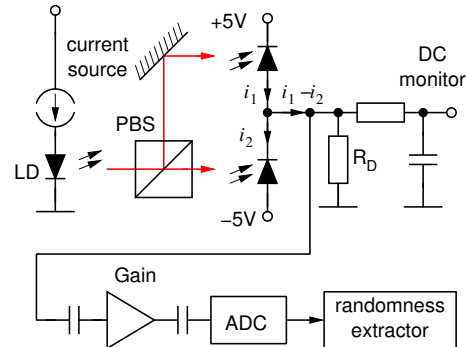


FIG. 1. Schematic of the quantum random number generator. A polarizing beam splitter (PBS) distributes light from a 780 nm laser equally onto two photodiodes, generating photocurrents i_1 and i_2 . The current difference $i_1 - i_2$ is amplified, digitized, and processed to generate random numbers.

cient randomness extractor, we obtain an unbiased, uncorrelated stream of random bits at a high rate.

II. IMPLEMENTATION

Figure 1 schematically shows the setup of our QRNG. A continuous wave laser (wavelength 780 nm) is used as the local oscillator (LO) for the vacuum fluctuations entering the beam splitter at the empty port. The output of the beam splitter is directed onto two photodiodes, and the photocurrent difference is processed further. This setup is known as a balanced homodyne detector^{31,32} and maps the electrical field in the second mode entering the beam splitter to the photocurrent difference $i_1 - i_2$. Here, the second input port is empty, so the homodyne measurement is probing the vacuum state of the electromagnetic field. This field fluctuates³³, and is used as the source of randomness. As the vacuum field is independent of external physical quantities, it can not be tampered with. Since the optical power impinging on the two photodiodes is balanced, any power fluctuation in the local oscillator will be simultaneously detected, and therefore cancel in the photocurrent difference^{32,34}. In an alternative view, the laser beam can be seen as generating photocurrents i_1, i_2 with a shot noise power proportional

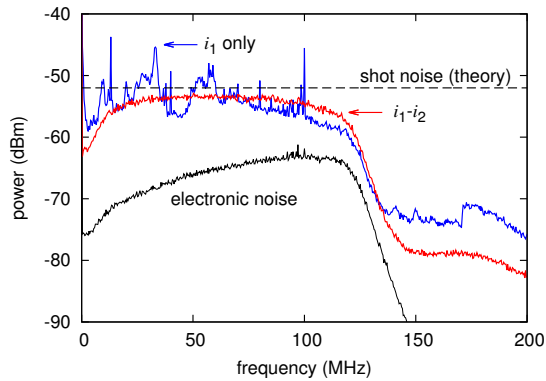


FIG. 2. Amplified noise levels measured into a resolution bandwidth $B = 1$ kHz. The total noise is measured from the photocurrent difference $i_1 - i_2$ with equal optical power impinging on both photodiodes and approaches the theoretical shot noise level of -52 dBm (dashed trace) given by (1). The current i_1 of a single photodiode reveals colored classical noise. The electronic noise is measured without any optical input.

to the average optical power. The shot noise currents from the diodes add up as they are uncorrelated, while amplitude fluctuations in the laser intensity (referred to as classical noise) do not affect the photocurrent difference.

The power of the two output ports is balanced by rotating the laser diode in front of a polarizing beam splitter (PBS). Light leaving the PBS is detected by a pair of reverse biased silicon pin photodiodes (Hamamatsu S5972) connected in series to perform the current subtraction. The balancing of photocurrents is monitored by observing the voltage drop across a resistor R_{DC} providing a DC path from the common node to ground. We achieve a 50 dB rejection ratio of the classical noise from the laser intensity fluctuations by careful balancing. The fluctuations $\Delta(i_1 - i_2)$ above 20 MHz are amplified by a transimpedance amplifier (Analog Devices AD8015) followed by two wideband RF gain blocks (Mini Circuits MAR-6). The entire amplifier chain has a calculated effective transimpedance of $R_{\text{eff}} \approx 540 \pm 118$ k Ω .

To ensure that the fluctuations at the amplifier output are dominated by quantum noise, the spectral power density is measured (see Fig. 2). With an optical power of 3.1 mW received by each photodiode corresponding to an average photocurrent $I = 1.7$ mA, we observe a noise power of $P = -53.5$ dBm (at 75 MHz) in a bandwidth of $B = 1$ kHz. This is about 1.5 dB lower than the theoretically expected shot noise value (dashed trace)

$$P = \frac{4eIBR_{\text{eff}}^2}{Z} \approx -52 \text{ dBm}, \quad (1)$$

where e is the electron charge and $Z = 50 \Omega$ the load impedance.³⁵ The difference is compatible with uncertainties in determining the transimpedance of the amplifier. The measured total noise has a relatively flat power

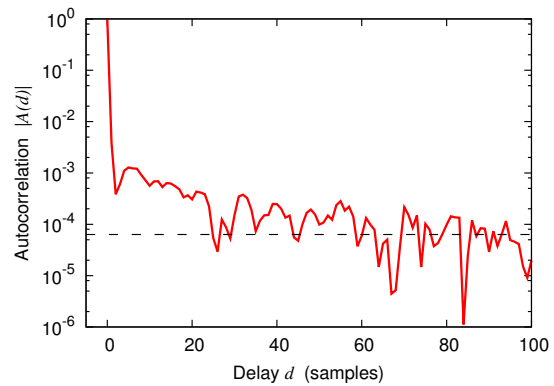


FIG. 3. Autocorrelation of the total noise signal sampled at 60 MHz, computed over 10^9 samples (solid line), compared with the 2σ confidence level (dashed line).

density in the range of 20 to 120 MHz, with high pass filters in the circuit suppressing low frequency fluctuations. The high end of the pass band is defined by the cutoff frequency of the amplifier. To illustrate the effectiveness of removing classical noise in the photocurrents, the spectral power density of the photocurrent generated from a single diode is also shown. Strong spectral peaks at various radio frequencies appear to enter the system probably via the laser diode current. For completeness, the spectral power density of the electronic noise is recorded without any optical input and found to be at least 10 dB below the total noise level, i.e., the total noise is dominated by quantum fluctuations.

The amplified total noise is digitized into signed 16 bit words x_i at a sampling rate of 60 MHz with an analog to digital converter (ADC, Analog Devices AD9269-65). The sampling rate is lower than the cut-off frequency of the noise signal to avoid temporal correlation between samples. As shown in Fig. 3, the normalized autocorrelation

$$A(d) = \langle x_i x_{i+d} \rangle_n / \langle x_i^2 \rangle_n \quad (2)$$

evaluated over $n = 10^9$ samples shows that the absolute value of the autocorrelation $|A(d)|$ for non-zero delay ($d > 0$) is below 1.2×10^{-3} , which is slightly smaller than what has been observed in other experiments.^{23,36,37} The residual correlation above the 2σ confidence level for $d \lesssim 60$ is a consequence of the finite bandwidth of the signal, as stated by the Wiener-Khinchin theorem.

III. ENTROPY ESTIMATION

The total noise measured before the ADC contains both quantum and electronic noise. To determine how much randomness from non-classical origin can be safely extracted, it is necessary to estimate the entropy $H(X_q)$ contributed by the quantum process.

Therefore, we assume that the measured total noise signal $X_t = X_q + X_e$ is the sum of independent ran-

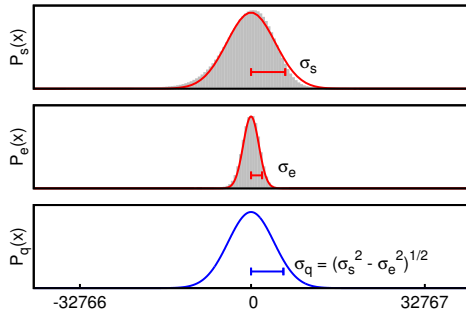


FIG. 4. Probability distribution of the measured total noise with variance σ_t^2 (a), electronic noise with variance σ_e^2 (b), and the estimated quantum noise with variance σ_q^2 (c). The filled areas in (a), (b) show the actual measurements over 10^9 samples, the solid lines fit to Gaussian distributions.

dom variables X_q for the quantum noise, and X_e for the electronic noise which includes the photodetector, amplifier and digitizer noise^{22,37}. All three variables X_q , X_e and X_t are assumed to have discrete values between -2^{15} and $2^{15} - 1$. We take the worst case scenario that an adversary has full knowledge of the electronic noise, i.e., is able to predict the exact outcome of X_e at any moment. In this case, the amount of quantum-based randomness in the acquired total noise signal is quantified by the conditional entropy $H(X_t|X_e)$, i.e., the entropy in the total signal, given full knowledge of the electronic noise X_e . As the variables are assumed to be additive and independent, the conditional entropy is $H(X_t|X_e) = H(X_q + X_e|X_e) = H(X_q|X_e) = H(X_q)$.

The variance of the total noise, σ_t^2 , is given by the sum of the variances σ_q^2 for the quantum noise, and σ_e^2 for the electronic noise. Over 10^9 samples, we find $\sigma_t = 4504.41$ and $\sigma_e = 1481.8$, measured with the laser switched off (see Fig. 4). Note that for the total noise, the observed distribution is slightly skewed compared to a Gaussian distribution [solid line in Fig. 4(a)], possibly due to a distortion in the digitizer. Assuming the quantum noise X_q has a Gaussian distribution³³, we would assign a variance $\sigma_q^2 = \sigma_t^2 - \sigma_e^2 \approx 4253.7^2$. To estimate the entropy for a Gaussian distribution, we use the Shannon entropy

$$H_S(X_q) = \sum_{x=-2^{15}}^{2^{15}-1} -p_q(x) \log_2 p_q(x), \quad (3)$$

where $p_q(x)$ is the probability distribution of the quantum noise X_q . Since $\sigma_q \gg 1$, $H_S(X_q)$ can be well approximated by

$$\int_{-\infty}^{+\infty} -f(x) \log_2 f(x) dx = \log_2(\sqrt{2\pi e} \sigma_q), \quad (4)$$

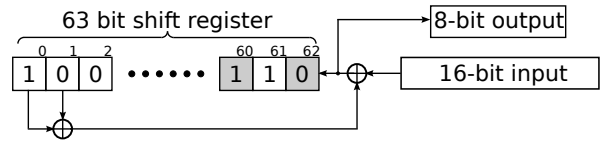


FIG. 5. Schematic of a LFSR-based randomness extractor. Eight bits (from the shaded positions) are extracted for every 16 bits of input.

where $f(x)$ is a Gaussian probability density function with variance σ_q^2 , and e the base of the natural logarithm³⁸. This yields 14.1 bits of entropy per 16 bit sample. We also evaluate the min-entropy of this distribution,

$$H_\infty(X_q) = -\log_2(\max[p_q(x)]) \approx \log_2(\sqrt{2\pi} \sigma_q), \quad (5)$$

where $\max[p_q(x)]$ is the maximum value of the probability distribution of X_q . This yields a min-entropy of 13.4 bits per 16 bit sample.

The Shannon entropy $H_S(X_q)$ serves as an upper bound of extractable randomness, while the min-entropy sets a lower bound, i.e. the least amount of randomness possessed by each sample. An alternative estimation of the entropy in X_q assumes that electronic noise is not only known to a third party, but also could be tampered with^{19,36,39}.

IV. RANDOMNESS EXTRACTION

In many applications, random numbers are required to be not only unpredictable, but also uniformly distributed. As such, the raw ADC output cannot be directly used. Randomness extractors convert non-uniformly distributed raw data into a uniformly distributed binary stream without correlations⁴⁰. Although there is no deterministic universal randomness extractor⁴⁰, various practical implementations have been reported. Examples are Trevisan's extractor, a Toeplitz hashing extractor³⁷, random matrix multiplications^{22,41}, or a family of secure hashing algorithms (SHA)¹⁸.

In this work, we use a randomness extractor based on a Linear Feedback Shift Register (LFSR) as shown in Fig. 5, equivalent to a cyclic redundancy check (CRC)⁴². The LFSRs are well known for generating long pseudo-random streams with little computational resources, and are in widespread use in communication applications for spectrum whitening⁴³⁻⁴⁷.

We use a maximum length LFSR with 63 cells and a two-element feedback path. Its state at any time t is a

row vector S_t of 63 bits, with a recursion relation

$$\begin{aligned}
 S_{t+1} &= S_t M + R_t \quad (6) \\
 &= (s_0, s_1, s_2, \dots, s_{62}) \begin{pmatrix} 0 & 0 & \dots & 0 & 1 \\ 1 & 0 & \dots & 0 & 1 \\ 0 & 1 & \dots & 0 & 0 \\ \vdots & \vdots & \ddots & \vdots & \vdots \\ 0 & 0 & \dots & 1 & 0 \end{pmatrix} \\
 &\quad + (0, 0, 0, \dots, 0, r_t) \\
 &= (s_1, s_2, s_3, \dots, s_{62}, s_0 + s_1 + r_t),
 \end{aligned}$$

where an elementary addition represents a binary xor, and a multiplication a binary and operation.

The 63×63 matrix M represents the shift and feedback operation on the LFSR state. The addition of row vector R_t describes the injection of one raw random bit r_t into S_t . After n cycles, the LFSR state becomes

$$S_{t+n} = S_t M^n + \underbrace{R_t M^{n-1} + \dots + R_{t+n-1}}_A. \quad (7)$$

Row vector A can be expressed as a matrix product

$$A = (r_t, r_{t+1}, \dots, r_{t+n-1}) T, \quad (8)$$

with

$$T = \begin{pmatrix} S' M^{n-1} \\ S' M^{n-2} \\ \vdots \\ S' I \end{pmatrix}, \quad S' = (0, 0, \dots, 0, 1). \quad (9)$$

Matrix T in (9) is a 63×63 Toeplitz matrix with rows generated from a LFSR sequence (6) with $R_t = 0$ and initial state $S_t = S'$. It was shown that multiplying an input stream by such a Toeplitz matrix can be used as a hashing function that generates an almost-uniform output⁴³.

In our setup, we serially inject the 16 bits from each ADC output word into the LFSR, but extract only 8 bits s_i provided by stream S_t (at positions 62, 60, \dots 48 after the injection) in a parallelized topology. This is equivalent to a privacy amplification process⁴⁸, and ensures that no residual correlations due to the non-uniform input distribution or any classical noise that may be known to an adversary are present in the output stream, because the extraction ratio of 50% is lower than the $13.4/16 \approx 84\%$ allowed by the min entropy (5).

A merit of this extractor is its low complexity. Unlike many other secure hashing algorithms, it can be easily implemented either in high speed or low power technology. Therefore, the extraction process does not limit the random number generation rate. This scheme can be parallelized using 126 register cells, capable of receiving up to 63 injected raw bits per clock cycle while still following the extractor equation (6). With a CPLD operating at a clock frequency of 400 MHz, this algorithm would be able to process up to 25×10^9 raw input bits per second.

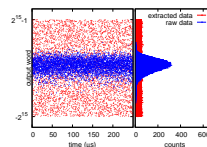


FIG. 6. Distribution of random data before (blue) and after (red) the randomness extractor, shown in time domain (left) and histogram (right).

V. PERFORMANCE

To evaluate the quality of the extracted random numbers, we apply two suites of randomness tests: the statistical test suite from NIST⁴⁹, and the “Die-harder” randomness test battery⁵⁰. The output of our RNG passed both tests consistently when evaluated over a sample of 400 Gigabit in the sense that occasional weak outcomes of some tests do not repeat.

Our implementation has an output rate of about 480 Mbit/s of uniformly distributed random bits, with the digitizer unit sampling at 60 MHz and randomness extraction ratio of 50%; this is limited by the speed of the data transmission protocol (USB2.0). While significantly higher generation rates have been reported recently^{17,23,25}, our design in comparison is simpler both in hard- and software implementation. With moderate effort, our random number generation rate can be greatly increased by extending the bandwidth of the photodiodes, amplifiers, and digitizer devices, while maintaining the relatively simple randomness extraction mechanism. Practically, the resolution-bandwidth product of the ADC limits the random bit generation rate.

VI. CONCLUSION

In summary, we demonstrated a random number generation scheme by measuring the vacuum fluctuations of the electromagnetic field. By estimating the amount of usable entropy from quantum noise and using an efficient randomness extractor based on a linear feedback shift register, we can generate uniformly distributed random numbers at a high rate from a fundamentally unpredictable quantum measurement.

We acknowledge the support of this work by the National Research Foundation (partly under grant No. NRF-CRP12-2013-03) & Ministry of Education in Singapore, partly through the Academic Research Fund MOE2012-T3-1-009.

- ¹N. Gisin, G. Ribordy, W. Tittel, and H. Zbinden, *Rev. Mod. Phys.* **74**, 145195 (2002).
- ²N. Metropolis, *Los Alamos Science* **15**, 125 (1987).
- ³F. Galton, *Nature* **42**, 1314 (1890).
- ⁴B. Jun and P. Kocher, “The intel random number generator,” *Tech. Rep. (Cryptography Research Inc., 1999)*.
- ⁵M. Gude, *Frequenz* **39**, 187 (1985).
- ⁶A. Figotin, I. Vitebskiy, V. Popovich, G. Stetsenko, S. Molchanov, A. Gordon, J. Quinn, and N. Stavarakas, “Random number generator based on the spontaneous alpha-decay,” (2004), uS Patent 6,745,217.
- ⁷M. Stipcevic and B. M. Rogina, *Rev. Sci. Instrum.* **78**, 045104 (2007).
- ⁸M. A. Wayne, E. R. Jeffrey, G. M. Akselrod, and P. G. Kwiat, *Journal of Modern Optics* **56**, 516 (2009).
- ⁹M. Fürst, H. Weier, S. Nauerth, D. G. Marangon, C. Kurtsiefer, and H. Weinfurter, *Optics Express* **18**, 13029 (2010).
- ¹⁰M. A. Wayne and P. G. Kwiat, *Opt. Express* **18**, 9351 (2010).
- ¹¹M. Wahl, M. Leifgen, M. Berlin, T. Rohlicke, H.-J. Rahn, and O. Benson, *Applied Physics Letters* **98**, 171105 (2011).
- ¹²Y.-Q. Nie, H.-F. Zhang, Z. Zhang, J. Wang, X. Ma, J. Zhang, and J.-W. Pan, *Applied Physics Letters* **104**, 051110 (2014).
- ¹³M. Ren, E. Wu, Y. Liang, Y. Jian, G. Wu, and H. Zeng, *Physical Review A* **83**, 023820 (2011).
- ¹⁴T. Jennewein, U. Achleitner, G. Weihs, H. Weinfurter, and A. Zeilinger, *Review of Scientific Instruments* **71**, 1675 (2000).
- ¹⁵A. Stefanov, N. Gisin, O. Guinnard, L. Guinnard, and H. Zbinden, *Journal of Modern Optics* **47**, 595 (2000).
- ¹⁶D. Frauchiger and R. Renner, *Proc. SPIE* **8899**, 88990S (2013).
- ¹⁷C. R. S. Williams, J. C. Salevan, X. Li, R. Roy, and T. E. Murphy, *Optics Express* **18**, 23584 (2010).
- ¹⁸C. Gabriel, C. Wittmann, D. Sych, R. Dong, W. Mauerer, U. L. Andersen, C. Marquardt, and G. Leuchs, *Nature Photon* **4**, 711715 (2010).
- ¹⁹T. Symul, S. M. Assad, and P. K. Lam, *Applied Physics Letters* **98**, 231103 (2011).
- ²⁰Y. Shen, L. Tian, and H. Zou, *Physical Review A* **81**, 063814 (2010).
- ²¹I. Kanter, Y. Aviad, I. Reidler, E. Cohen, and M. Rosenbluh, *Nature Photon* **4**, 5861 (2009).
- ²²B. Sanguinetti, A. Martin, H. Zbinden, and N. Gisin, *Phys. Rev. X* **4**, 031056 (2014).
- ²³Y.-Q. Nie, L. Huang, Y. Liu, F. Payne, J. Zhang, and J.-W. Pan, *Review of Scientific Instruments* **86**, 063105 (2015).
- ²⁴B. Qi, Y.-M. Chi, H.-K. Lo, and L. Qian, *Opt. Lett.* **35**, 312 (2010).
- ²⁵F. Xu, B. Qi, X. Ma, H. Xu, H. Zheng, and H.-K. Lo, *Optics Express* **20**, 12366 (2012).
- ²⁶C. Abellán, W. Amaya, M. Jofre, M. Curty, A. Acn, J. Capmany, V. Pruneri, and M. W. Mitchell, *Optics Express* **22**, 1645 (2014).
- ²⁷C. Abellán, W. Amaya, D. Mitrani, V. Pruneri, and M. W. Mitchell, *Phys. Rev. Lett.* **115**, 250403 (2015).
- ²⁸Z. L. Yuan, M. Lucamarini, J. F. Dynes, B. Frhlich, A. Plews, and A. J. Shields, *Applied Physics Letters* **104**, 261112 (2014).
- ²⁹H. Zhou, X. Yuan, and X. Ma, *Physical Review A* **91**, 062316 (2015).
- ³⁰M. Jofre, M. Curty, F. Steinlechner, G. Anzolin, J. P. Torres, M. W. Mitchell, and V. Pruneri, *Optics Express* **19**, 20665 (2011).
- ³¹E. Jakeman, C. Oliver, and E. Pike, *Advances in Physics* **24**, 349 (1975).
- ³²H. P. Yuen and V. W. Chan, *Optics Letters* **8**, 177 (1983).
- ³³R. J. Glauber, *Phys. Rev.* **131**, 2766 (1963).
- ³⁴B. L. Schumaker, *Optics Lettes* **9**, 189 (1984).
- ³⁵W. Schottky, *Annalen der Physik* **362**, 541567 (1918).
- ³⁶M. W. Mitchell, C. Abellan, and W. Amaya, *Phys. Rev. A* **91**, 012314 (2015).
- ³⁷X. Ma, F. Xu, H. Xu, X. Tan, B. Qi, and H.-K. Lo, *Phys. Rev. A* **87**, 062327 (2013).
- ³⁸One can show that $|H(X_q) - H'(X_q)| < \log_2(\sqrt{2\pi\sigma_q})/(\sqrt{2\pi\sigma_q}) \approx 0.0013$ bit for $\sigma_q = 4108$.
- ³⁹J. Y. Haw, S. M. Assad, A. M. Lance, N. H. Y. Ng, V. Sharma, P. K. Lam, and T. Symul, *Phys. Rev. Applied* **3**, 054004 (2015).
- ⁴⁰M. Santha and U. V. Vazirani, *J. Comput. Syst. Sci.* **33**, 75 (1986).
- ⁴¹D. Frauchiger, R. Renner, and M. Troyer, arXiv:1311.4547 [quant-ph] (2013), 1311.4547.
- ⁴²W. W. Peterson and D. T. Brown, *Proceedings of the IRE* **49**, 228 (1961).
- ⁴³H. Krawczyk, *Advances in Cryptology CRYPTO 94*, 129139 (1994).
- ⁴⁴E. Barkan, E. Biham, and N. Keller, *J. Cryptol* **21**, 392429 (2007).
- ⁴⁵T. E. Tkacik, in *Cryptographic Hardware and Embedded Systems - CHES 2002*, Lecture Notes in Computer Science, Vol. 2523, edited by B. S. Kaliski, c. K. Koç, and C. Paar (Springer Berlin Heidelberg, 2003) pp. 450–453.
- ⁴⁶S. Wells and D. Ward, “Random number generator with entropy accumulation,” (2004), uS Patent 6,687,721.
- ⁴⁷K. Tsoi, K. Leung, and P. Leong, *Computers Digital Techniques, IET* **1**, 349 (2007).
- ⁴⁸C. H. Bennett, G. Brassard, C. Crepeau, and U. M. Maurer, *IEEE Transactions on Information Theory* **41**, 1915 (1995).
- ⁴⁹A. Rukhin, J. Soto, J. Nechvatal, M. Smid, E. Barker, S. Leigh, M. Levenson, M. Vangel, D. Banks, A. Heckert, J. Dray, and S. Vo, *A Statistical Test Suite for Random and Pseudorandom Number Generators for Cryptographic Applications*, National Institute of Standards and Technology (2010).
- ⁵⁰D. B. Robert G. Brown, Dirk Eddelbuettel, “Dieharder: A random number test suite,” (2004).